Journal of Cell Science 111, 1567-1574 (1998)
Printed in Great Britain © The Company of Biologists Limited 1998
JCS4512

Characterizing titin's I-band Ig domain region as an entropic spring

Wolfgang A. Linke[1,*], Marc R. Stockmeier[1], Marc Ivemeyer[1], Hiltraud Hosser[2] and Peter Mundel[2]

[1]Institute of Physiology II, University of Heidelberg, Im Neuenheimer Feld 326, D-69120 Heidelberg, Germany
[2]Institute of Anatomy I, University of Heidelberg, Im Neuenheimer Feld 307, D-69120 Heidelberg, Germany
*Author for correspondence (e-mail: wolfgang.linke@urz.uni-heidelberg.de)

Accepted 25 March; published on WWW 14 May 1998

SUMMARY

The poly-immunoglobulin domain region of titin, located within the elastic section of this giant muscle protein, determines the extensibility of relaxed myofibrils mainly at shorter physiological lengths. To elucidate this region's contribution to titin elasticity, we measured the elastic properties of the N-terminal I-band Ig region by using immunofluorescence/immunoelectron microscopy and myofibril mechanics and tried to simulate the results with a model of entropic polymer elasticity. Rat psoas myofibrils were stained with titin-specific antibodies flanking the Ig region at the N terminus and C terminus, respectively, to record the extension behaviour of that titin segment. The segment's end-to-end length increased mainly at small stretch, reaching ~90% of the native contour length of the Ig region at a sarcomere length of 2.8 μm. At this extension, the average force per single titin molecule, deduced from the steady-state passive length-tension relation of myofibrils, was ~5 or 2.5 pN, depending on whether we assumed a number of 3 or 6 titins per half thick filament. When the force-extension curve constructed for the Ig region was simulated by the wormlike chain model, best fits were obtained for a persistence length, a measure of the chain's bending rigidity, of 21 or 42 nm (for 3 or 6 titins/half thick filament), which correctly reproduced the curve for sarcomere lengths up to 3.4 μm. Systematic deviations between data and fits above that length indicated that forces of >30 pN per titin strand may induce unfolding of Ig modules. We conclude that stretches of at least 5-6 Ig domains, perhaps coinciding with known super repeat patterns of these titin modules in the I-band, may represent the unitary lengths of the wormlike chain. The poly-Ig regions might thus act as compliant entropic springs that determine the minute levels of passive tension at low extensions of a muscle fiber.

Key words: Connectin, Entropic elasticity, Immunoelectron microscopy, Immunoglobulin domains, Passive tension, Wormlike chain

INTRODUCTION

Over the past few years, much has been learned about the elastic properties of titin (also called connectin), the giant protein primarily responsible for the development of passive tension during stretch of relaxed muscle fibers (Labeit et al., 1997; Maruyama, 1997; Erickson, 1997). The >3,000 kDa titin polypeptide chain spans half-sarcomeres from the Z-disk to the M-line, but only the molecule's I-band portion is functionally extensible (Fürst et al., 1988; Itoh et al., 1988; Trombitas et al., 1991) and involved in the generation of passive force (Horowits et al., 1986; Wang et al., 1991). I-band titin elasticity has become a matter of particular interest following the determination of titin's amino acid sequence by Labeit and Kolmerer (1995), who showed that the elastic segment of the polypeptide consists of two distinct structural motif types, poly-immunoglobulin (Ig) domains and a region of as yet unknown secondary structure, termed the PEVK domain (Fig. 1); both motif types are expressed in muscle tissue-specific length isoforms and are important for titin elasticity (Labeit and Kolmerer, 1995). Uncovering the contribution of each of these titin segments to the elastic properties of the sarcomere is an important aim of current research on titin.

Immunofluorescence and immunoelectron microscopic studies on stretched sarcomeres labeled with titin-specific antibodies have presented first evidence for a differential extensibility of the two I-band titin motifs (Linke et al., 1996; Gautel and Goulding, 1996). It was shown that the Ig domain segments elongate, probably by straightening out, predominantly within a low sarcomere length (SL) range where passive force is very small, whereas the PEVK domain is responsible for length gains at moderate SLs where passive force increases more steeply (Fig. 1). Only at extreme sarcomere extensions may unfolding of individual Ig domains occur (Granzier et al., 1996; Linke et al., 1996), a mechanism recently demonstrated in in-vitro mechanical experiments with single titin molecules (Kellermayer et al., 1997; Rief et al., 1997; Tskhovrebova et al., 1997). Currently, I-band titin is understood to represent a highly nonlinear spring composed of at least two elastic elements in series.

Although the precise molecular mechanism of titin elasticity remains to be discovered, the results of the single-molecule experiments have suggested that, at lower stretch, the PEVK element and the Ig domain chain (before the unfolding of modules) may generate force by an 'entropic spring' mechanism (Kellermayer et al., 1997; Tskhovrebova et al.,

1997). To test this concept, for the Ig region, to begin with, under conditions more closely resembling those found in the sarcomere, we have combined immunofluorescence and immunoelectron microscopy with isolated myofibril mechanics to determine the force-extension relation of poly-Ig segments of psoas muscle titin. The results were then simulated by recent entropic elasticity models, based on algorithms developed to describe the mechanical properties of a polymer chain (Marko and Siggia, 1995; Smith et al., 1996). We find that over the entire physiological SL range, the elastic properties of the poly-Ig segment can be simulated correctly with a wormlike chain (WLC) model. Based on these results, we discuss implications for the understanding of titin elasticity in skeletal muscle fibers.

MATERIALS AND METHODS

Myofibril preparation

Single myofibrils were isolated from freshly excised male Wistar rat psoas muscle essentially as described (Linke et al., 1997). Briefly, thin muscle strips were dissected and skinned in ice-cold rigor solution containing 0.5% Triton X-100 for a minimum of 4 hours. The skinned strips were minced and homogenized in rigor. A drop of the suspension was placed on a coverslip, and a myofibril adhering lightly to the glass surface was selected for an experiment under a Zeiss Axiovert inverted microscope. Experiments were performed at room temperature. Solutions had an ionic strength of 200 mM, pH 7.1, and were supplemented with protease inhibitor leupeptin or complete protease inhibitor cocktail tablets (Linke et al., 1997), aimed to prevent titin degradation. To test for the preservation of titin, we prepared 2% agarose-strengthened SDS-polyacrylamide gels (Tatsumi and Hattori, 1995) as described by Linke et al. (1997), and found that most of the titin in suspensions of rat psoas myofibrils remained in its undegraded T1 form (Fig. 2). Frequently, a faint T2 band co-migrated with the T1 band, indicating some damage, but the T1:T2 ratio was typically between 4:1 and 5:1 (measured with AIDA software, Raytest). Hence, the magnitude of degradation was no larger than ~20%.

Titin antibodies

The monoclonal titin antibody T12 was kindly provided by Dr Fürst (Fürst et al., 1988). The polyclonal antibody N2-A was raised to expressed titin sequences from the N2-A titin segment as described (Linke et al., 1996); it was developed in rabbits and affinity-purified by Eurogentec (Belgium).

Immunofluorescence microscopy

Immunofluorescence measurements on stretched myofibrils were performed with the aid of hydraulic micromanipulators (Narishige, Japan) under the inverted microscope (epifluorescence mode; ×100, 1.4 NA objective). The myofibril image was recorded with a sensitive CCD video camera (FK440, Völker, Maintal, Germany) and a 586 PC with frame grabber board (Vision-EZ, Data Translation). To increase resolution (~80 nm; Linke et al., 1997), three images at a given SL were recorded and automatically superimposed by using a feature of the software (GlobalLab Image, Data Translation). In a typical experimental protocol, a single myofibril was stretched in relaxing solution from slack SL to a desired length, was labeled with a primary antibody and, after washout, with TRITC-conjugated anti-mouse IgG (Sigma, no. T-5393) or Cy3-conjugated anti-rabbit IgG (Rockland, no. 3838). Myofibrils stained only with secondary antibody showed no fluorescence.

Immunoelectron microscopy

Psoas muscle stretched to different degrees in situ was excised from freshly killed rats previously perfused directly with a solution containing 4% paraformaldehyde. The preparation was processed for cryosectioning and immunolabeling with the titin antibodies and 10 nm gold particles essentially as described (Tokuyasu, 1989; Mundel et al., 1991). Electron micrographs were taken with a Philips EM 301 at 80 kV. The center of the nanogold particles was used to measure the distance of a given antibody epitope from the center of the Z-disk.

Passive tension recordings

A setup used to measure forces of isolated myofibrils has been

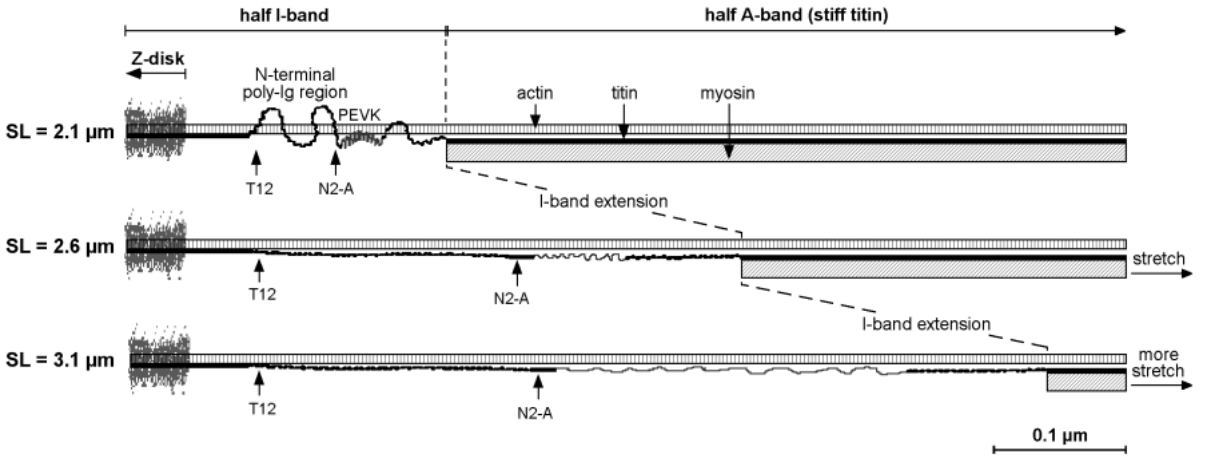

Fig. 1. Layout of psoas muscle titin in the half-sarcomere and extension behaviour during stretch (adapted from Linke et al., 1996, 1997). The epitope positions of the two titin antibodies used in this study, T12 and N2-A, are indicated below each panel. The functionally elastic I-band titin segment spans from the T12 epitope to the A/I junction. Two major structural motif types of the I-band, poly-Ig domain regions and a sequence rich in Pro, Glu, Val, and Lys residues, termed the PEVK domain, confer extensibility to titin (Labeit and Kolmerer, 1995; Linke et al., 1996). Top: Half-sarcomere at slack length. Middle: Moderately stretched half-sarcomere. The poly-Ig regions are straightened out, whereas the PEVK length has increased only little. Bottom: Half-sarcomere stretched to near the maximum length presumably reached under physiological conditions. The poly-Ig domain regions are fully straightened, whereas the PEVK domain is unraveled.

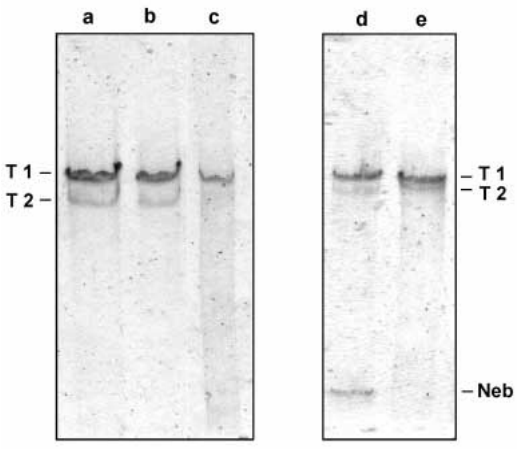

Fig. 2. 2% SDS-polyacrylamide gels of high molecular mass myofibrillar proteins (rat). (a) Psoas muscle fibers from rapidly excised and quick-frozen tissue. (b) Suspension of psoas myofibrils prepared from freshly excised and 4 hour-long skinned muscle. (c) For comparison, cardiac muscle tissue (right ventricle) from rapidly excised and quick-frozen heart. (d) Suspension of psoas myofibrils from freshly excised and 4 hour-long skinned muscle, but a different preparation from that in b. (e) Suspension of cardiac myofibrils from freshly excised and 4 hour-long skinned left ventricular tissue. In lanes d and e, less time was allowed for the migration of proteins than in the first three lanes, to visualize the ~800 kDa band for nebulin (Neb), which is expressed in skeletal muscle, but not in the heart. T1: band corresponding to native titin; T2: lower molecular mass titin band, which appears presumably due to proteolysis of native titin. In myofibrils from freshly excised tissue, used in this study for mechanical measurements, ~80% of titin remains in the T1 form. Altogether, preservation of titin is similar to that reported by Granzier and Irving (1995).

described (Linke et al., 1997). Briefly, each end of a specimen is attached with silicone adhesive (Dow Corning 3140/3145 RTV, 1:1 mixture) to a glass needle tip, one connected to a piezoelectric motor, the other to a home-built force transducer (sensitivity ~5 nN). SL can be measured with a 512-element linear photodiode array (Reticon) or the CCD camera, frame grabber and image analysis software. Data collection and simultaneous motor control are done with a 586 PC and National Instruments data aquisition board (PCI-MIO-16-E1) by using custom-written Labview software.

For the force measurements we used small bundles of 3-5 myofibrils, instead of single myofibrils, to improve signal-to-noise ratio particularly at the short SLs. Force was measured in non-antibody-labeled specimens. Typically, a relaxed preparation was stretched from slack length to a series of desired SLs. Stretch duration was ~10 seconds; the hold period between stretches (to wait for stress relaxation at constant length) was 1-2 minutes. Following stretch to a maximum length, the specimen was released in stages to slack SL. Force data were recorded every 4 milliseconds and stored in binary format; later they were median-filtered by using algorithms supplied by Labview. To obtain passive tension, the cross-sectional area of a specimen, assumed to have circular shape, was either inferred from the diameter of a myofibril bundle measured by phase-contrast microscopy (precision of specimen edge detection, two pixels, or, ~0.16 μm) or calculated by counting the number of myofibrils in a preparation and taking a value of 1.0 μm for the myofibrillar diameter (Bartoo et al., 1993; Linke et al., 1994). With both methods, results were similar within ±10%.

Calculations

The Ig-domain region of I-band titin was assumed to behave as a polymer chain, for which, in a standard WLC model (Bustamante et al., 1994; Marko and Siggia, 1995), the external force (*f*) is related to the fractional extension (*z*/*L*) by the relationship:

$$fA/(k_BT) = z/L + 1/(4(1 - z/L)^2) - 1/4, \quad (1)$$

where A is the persistence length, k_B is the Boltzmann constant, T is absolute temperature (in our experiments, 300 K), z is the end-to-end length of the WLC, and L is the contour length (end-to-end length of the chain stretched with 'infinite' force). We also applied another model of polymer-chain elasticity, the freely-jointed chain (FJC) model (Smith et al., 1996), which uses parameters similar to those used for the WLC model to describe the chain's elasticity. The force necessary to extend a single titin molecule's Ig segment was deduced from the passive tension-SL curve by using a value of 2.4×10^9 titins per mm^2 cross-sectional area (Higuchi et al., 1993), which is comparable to using a number of 6 titin strands per half thick filament (Whiting et al., 1989; Granzier and Irving, 1995). Similar calculations were also done by assuming a number of 3 titins per half thick filament (Maruyama, 1994). z could be measured as the distance between the T12 and the N2-A epitope. For L of the N-terminal Ig segment of native psoas muscle titin, we took a value of 225 nm, as estimated from the number of 50 domains (according to sequence data; Labeit and Kolmerer, 1995; Linke et al., 1996), multiplied by 4.5 nm for the (assumed) maximal domain spacing. An L value of ~225 nm was also deduced from the $f^{-1/2}$ vs z relation of the poly-Ig segment by applying WLC theory (cf. Fig. 7, inset). Calculation of A and curve fitting were done with Origin 5.0 software (Microcal), by using a nonlinear least-squares method (Levenberg-Marquardt algorithm).

RESULTS

Extension of the N-terminal poly-Ig chain

The extensibility of the N-terminal poly-Ig segment of psoas muscle titin was investigated by immunofluorescence microscopy in sarcomeres of single myofibrils stretched to varying degrees. Fig. 3 shows typical images of myofibrils

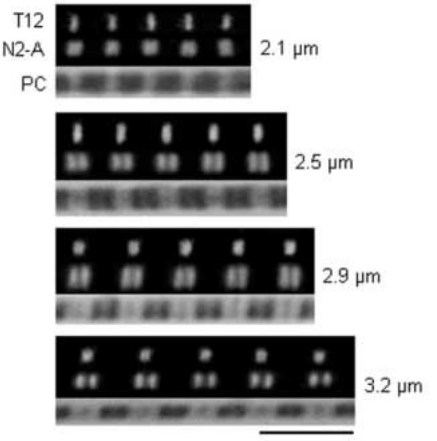

Fig. 3. Immunofluorescence images of single rat psoas myofibrils stretched to different sarcomere lengths (indicated on the right) and labeled with either the T12 or the N2-A titin antibody and fluorophore-conjugated secondary IgG antibody. All sarcomeres in a given myofibril show a characteristic staining pattern; the N2-A epitope translates away from the Z-disk upon sarcomere stretch. For comparison, phase-contrast (PC) images are shown at the bottom of each panel. Bar, 5 μm.

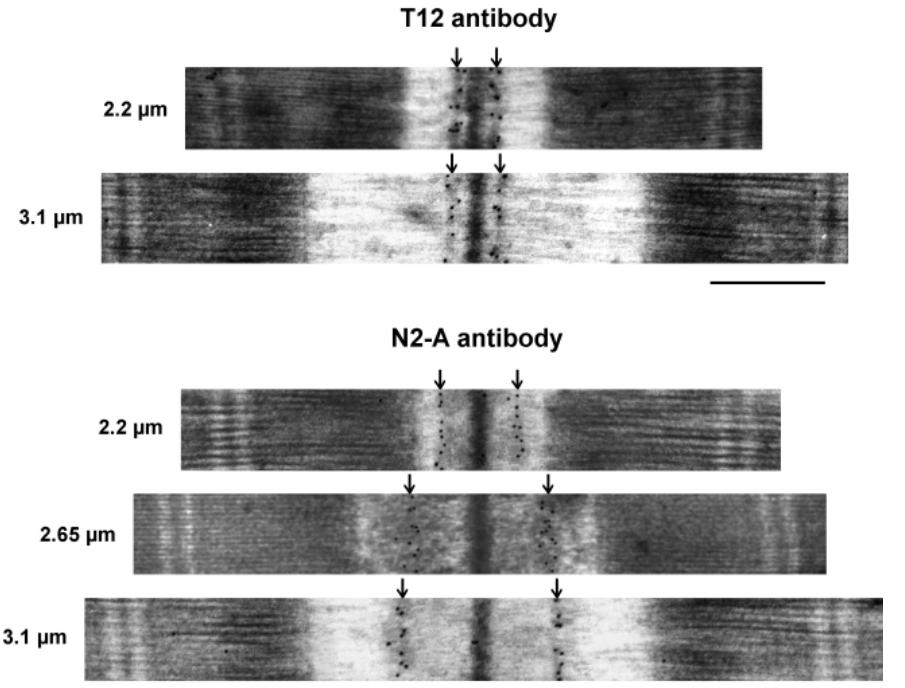

Fig. 4. Immunoelectron micrographs of stretched psoas muscle sarcomeres stained with the T12 or N2-A titin antibody. The nanogold particles indicate the respective epitope positions (arrows). The T12 epitopes barely move away from the Z-disk center, but the Z-line to N2-A distance increases greatly with stretch. Note that this increase takes place mainly at lower sarcomere extension. Bar, 0.5 µm.

extended to four different SLs and stained with the T12 or the N2-A antibody. The T12 epitopes on either side of the Z-disk appeared as two closely spaced stripes at long SLs (epitope-epitope spacing at 3.2 µm SL, 0.2-0.3 µm), but were frequently merged into one broader epitope at the shorter lengths, so that the immunofluorescence method did not provide enough resolution to determine the precise T12-N2-A distance. However, as reported earlier (Linke et al., 1996), this distance, representing the length of the Ig domain region, was found to increase mainly at lower stretch but little at higher extension.

An immunoelectron microscopical technique was employed to measure the SL-dependent spacing between the Z-disk center and the T12 and N2-A epitopes, respectively, with higher precision (Fig. 4). The T12 epitopes remained almost stationary relative to the Z-disk over the SL range investigated (2.0-3.1 µm), as expected from earlier work (e.g. Trombitas and Pollack, 1993). In contrast, the Z-disk center to N2-A distance increased greatly upon stretch from 2.0 to ~2.7 µm SL, but little with further extension to ~3.2 µm, the longest SL obtained for psoas myofibrils with the in-situ fixation technique applied. The results of the immunolabeling experiments are summarized in Fig. 5A. The T12 data points (EM results only) were fitted with a first-order regression curve that has a very flat slope, indicating that the contribution of the Z-disk-T12 segment to the extensibility of I-band titin is very small. As for N2-A, data from both the immunoelectron microscopic and the immunofluorescence measurements are shown. With both methods, results were similar within experimental error.

The T12 fit curve was then subtracted from the third-order regression curve for N2-A (EM) to obtain extension of the N-terminal poly-Ig region versus SL (Fig. 5B). Lengthening of the Ig domain segment was found to take place mainly at smaller extensions: at 2.1 µm SL, the region's end-to-end length was ~70 nm, or ~30% of its estimated native contour length (for calculations, see Materials and Methods), whereas at 2.8 µm it was ~200 nm (~90% of the contour length). Further stretch to 3.2 µm SL increased the end-to-end length to only ~215 nm (~95% of the contour length). Finally, judging from the immunofluorescence data, it was likely that the Ig segment's end-to-end length reached the contour length near 3.5 µm SL.

Force per titin

To determine the force-extension relation of a single titin's N-terminal poly-Ig region, it was necessary to obtain force per titin. We deduced this parameter from the quasi steady-state, passive length-tension curve of isolated psoas myofibrils (Fig. 6). In contrast to a recent study from our laboratory, in which we reported the passive tension curve of single myofibrils (Linke et al., 1996), we here recorded tension on small bundles of 3-5 myofibrils, to reliably detect the very low force levels at the short SLs. Except for the small forces now resolvable between slack length and ~2.5 µm SL (Fig. 6A), the tension values at a given SL (Fig. 6B) were similar to those measured in single myofibrils. To calculate force per single titin strand (see Materials and Methods), we used the following assumptions: (i) all titin molecules (1,000-2,000 parallel filaments per myofibril; cf. Linke et al., 1994) behave independently of one another and have comparable elastic properties; (ii) all parallel titin strands or titin segments within a molecule bear the same force at a given extension; the sum of these parallel forces is the force measured at the ends of the myofibril. With these assumptions, we calculate the force per titin strand to be ~5 or 2.5 pN at 2.8 µm SL, depending on whether we take a value of 3 or 6 titins per half thick filament (Fig. 6B, inset). At an SL of 3.2 µm, the force is ~20 (10) pN, and at 3.6 µm, it reaches 50 (25) pN.

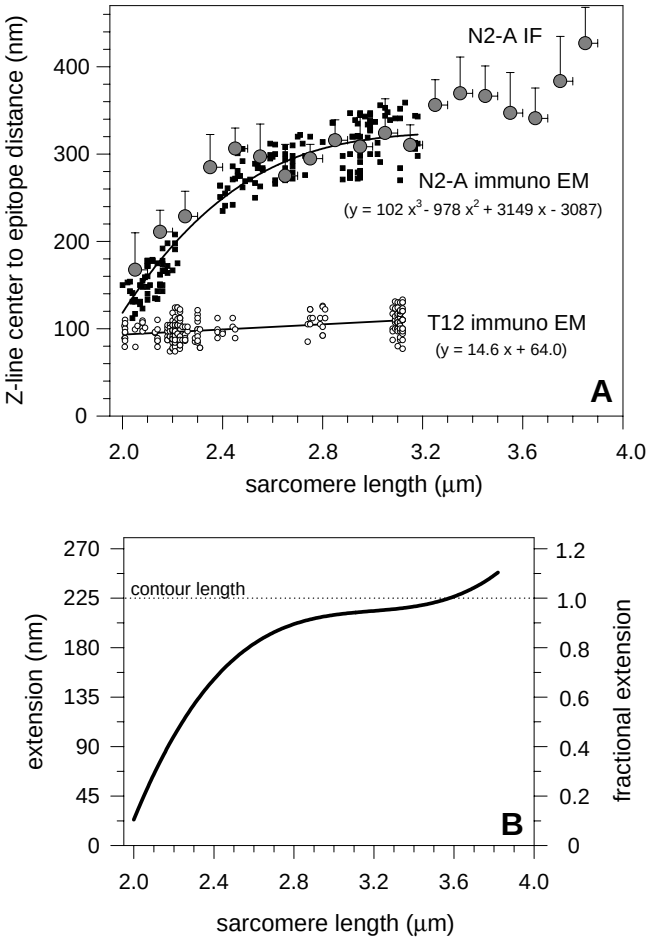

Fig. 5. Extension behaviour of the N-terminal poly-Ig segment. (A) Summary of results of immunolabeling experiments. Data points for the Z-line center to epitope spacing at different SLs, as determined by immunoelectron microscopy, are shown for both T12 (open circles) and N2-A (filled squares). The larger shaded circles and error bars indicate the mean distances from the Z-disk center and standard deviations (at 0.1 μm SL increments) for the N2-A epitope, measured by immunofluorescence microscopy (IF). Curve fitting parameters (EM data only) are also shown. (B) Extension of the N-terminal Ig domain segment vs SL. The left axis indicates absolute extension, the right axis fractional extension (relative to the poly-Ig region's estimated contour length of 225 nm; cf. Materials and Methods and Fig. 7, inset).

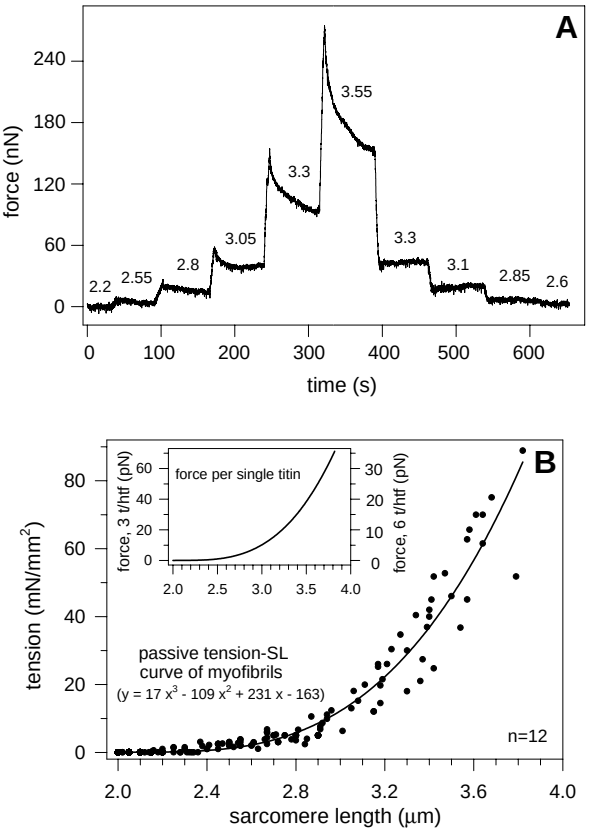

Fig. 6. Force-SL relations. (A) Original force trace from a stretch-release experiment with a preparation consisting of three myofibrils. To reduce noise, the data had been filtered with a rank-3 median filter supplied by Labview. The specimen was stretched in stages from slack SL (2.2 μm) to a series of desired length and was held at each length for ~1 minute to wait for stress relaxation (force decay at constant SL). Numbers above the tracing indicate SL during the hold periods. After stretch to a maximum SL, a stepwise release protocol was performed. Force became undetectable at ~2.6 μm SL, but the specimen slowly shortened further down to 2.22 μm. (B) Steady-state passive tension vs SL relation of isolated psoas myofibrils. Data points shown include only force values obtained during the first stretch of the altogether 12 specimens; some preparations were not extended to above 3.0 μm SL. The parameters used for the third-order regression of the experimental data are indicated. The inset shows force per single titin strand, extrapolated from the curve in the main figure by assuming a number of 3 titins (left axis) or 6 titins (right axis) per half thick filament (t/htf).

Modeling titin's Ig domain segment as a WLC

To define the elastic properties of the N-terminal poly-Ig segment, we plotted force per single titin strand versus fractional extension (Fig. 7). Force was found to be very low (<1.6 pN for 3 titins/half thick filament or half that value for a 6:1 ratio) up to a fractional extension of 0.8, reached at ~2.6 μm SL (cf. Fig. 5B). Above that length, force increased moderately up to 5 (2.5) pN at a fractional extension of 0.9, corresponding to ~2.8 μm SL. With fractional extension greater than 0.9, a steep force rise was apparent. However, the slope of the force-extension curve decreased again when the force reached values of several tens of picoNewtons.

The experimental data were then tried to be fitted with a standard WLC model of entropic elasticity (Bustamante et al., 1994; Marko and Siggia, 1995), which has been suggested to be a useful tool to describe the elastic properties of whole titin filaments at low to moderate extension (Kellermayer et al., 1997; Tskhovrebova et al., 1997). Best fits, faithfully reproducing the experimentally determined curve, were returned for a persistence length, *A*, of ~21 or ~42 nm (for 3 and 6 titins/half thick filament, respectively). The results are shown in Fig. 7. Importantly, to obtain good fits (χ^2 <1), we had to exclude the data for a fractional extension >0.96; otherwise, even the best fit did not correctly describe the measured force-extension curve at forces higher than 34 (17) pN. Such systematic deviations between fits and data at large extensions indicate the onset of structural alterations in the

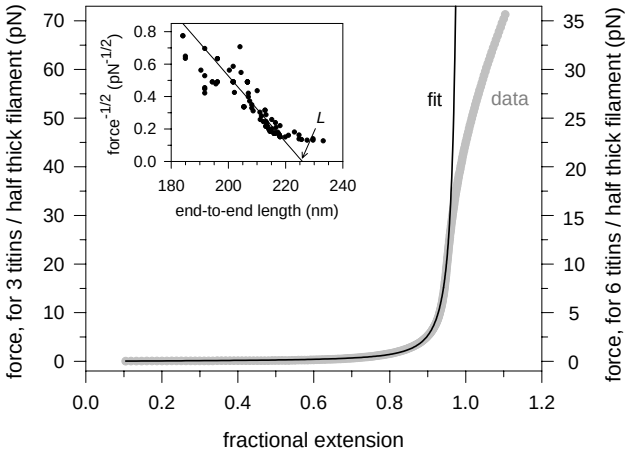

Fig. 7. Force vs fractional extension (thick shaded line) and fit according to the WLC model (thin black line) calculated for the N-terminal poly-Ig segment (psoas muscle) of a single titin molecule. A contour length of 225 nm was assumed. The experimental data could be fitted correctly for fractional extensions ≤0.96. Within this extension range, a best fit with the nonlinear least-squares regression method employed ($\chi^2 = 0.057$) returned a persistence length of 21 nm (assuming 3 titins per half thick filament) or 42 nm (assuming a 6:1 ratio). Systematic deviations between data and fits occurred for fractional extensions >0.96. Inset: $f^{-1/2}$ vs z plot for the poly-Ig region. Force per titin was deduced from the passive tension data (Fig. 6) by using a value of 1.2×10^9 titins per mm^2 cross-sectional area. z was obtained from the passive length-tension relation and the SL-extension curve shown in Fig. 5B. A linear fit to the force data at high extensions is extrapolated to the z axis to obtain the contour length (L).

molecule, in our case probably unfolding of individual Ig modules. We also applied another entropic elasticity model, the FJC model (Smith et al., 1996), but there were systematic deviations from the experimental data even at shorter fractional extensions. Thus, the WLC model was considered to be the 'gold standard' to describe the experimental findings.

Because the contour length of the WLC affects the above calculations (in which L was assumed to be 225 nm), we performed such calculations also with different L values ranging from 200 to 230 nm. For L <215 nm, there were large systematic deviations between data and fits, particularly above 85% fractional extension. L values of 215 and 220 nm resulted in best fits with persistence lengths of 27 (54) and 24 (48) nm, respectively (for 3 (6) titins/half thick filament), whereas calculations using L = 230 nm revealed an A value of ~15 (30) nm. However, with all of these assumed contour lengths, obvious deviations between data and fits occurred at low and high forces. Thus, the experimental data were apparently described best by the fit curve shown in Fig. 7. To further explore this issue, we used WLC theory to help identify the correct L value. This was done as suggested by Kellermayer et al. (1997), among others, by plotting force$^{-1/2}$ vs end-to-end length of the WLC at high extensions and applying a linear fit to the data (Fig. 7, inset). The extrapolated point of intersection of the fit curve with the extension axis at zero force$^{-1/2}$ indeed revealed a contour length of ~225 nm. We again took this result as a confirmation of the validity of the fit curve in Fig. 7.

DISCUSSION

Micromechanical studies on single isolated titin molecules have recently demonstrated that the Ig and/or fibronectin domains, which represent the main structural motif types of the titin chain (Improta et al., 1996) and together, make up nearly 90% of the polypeptide's mass (Labeit and Kolmerer, 1995), can unfold under high external forces (Kellermayer et al., 1997; Rief et al., 1997; Tskhovrebova et al., 1997). However, at lower forces, those likely to be relevant during normal functioning of skeletal muscle, another mechanism, driven by thermal energy, has been suggested to account for the elasticity of titin and was termed 'entropic spring' mechanism (summarized by Erickson, 1997). Whereas much of our understanding about titin elasticity has come from these single-molecule experiments, the question remains as to whether the elastic properties of isolated titin strands examined in vitro are comparable to those of titin filaments in situ, which interact with other sarcomeric proteins and perhaps with one another (for reviews, see Trinick, 1994; Labeit et al., 1997; Maruyama, 1997). Most importantly, titin is functionally extensible only along part of its I-band section (Trombitas and Pollack, 1993; Wang et al., 1993; Linke et al., 1997), a molecular segment with heterogeneous structure that is primarily made up of two longer stretches of Ig repeats separated by the PEVK domain (Labeit and Kolmerer, 1995; cf. Fig. 1). To uncover the molecular basis of titin elasticity, it is therefore desirable to 'functionally dissect' I-band titin into the structurally distinct regions and measure the elastic properties of each segment.

Of the two principal structural motif types of I-band titin, the PEVK domain appears to account for the extensibility of skeletal muscle titin at moderate sarcomere extensions where significant passive tension develops (Linke et al., 1996). The mechanism of PEVK-segment elasticity is still unknown, and proposals that the 'entropic spring' concept can be applied to this titin region (Kellermayer et al., 1997; Tskhovrebova et al., 1997) need to be tested in the environment of the sarcomere. The other major components of I-band titin, the poly-Ig segments, may be responsible for sarcomere elongation predominantly at low extension (Gautel and Goulding, 1996; Linke et al., 1996), as now confirmed in this study. Probably, the Ig domain segments elongate by straightening out from a partially collapsed state (Erickson, 1994; Granzier et al., 1996; Linke et al., 1996). Then, according to the entropic spring concept, to extend the segments by an external force it would be necessary to counteract the forces brought about by exposure of the chains to thermal fluctuations. The pulling forces needed greatly depend on the ratio between the polymer's contour length and its persistence length (a measure of bending rigidity): the larger this ratio, the stiffer the spring.

The present study focussed on the N-terminal Ig domain region of psoas muscle titin to examine, whether the entropic spring concept can indeed explain the elastic properties of this region. By employing immunofluorescence and immunoelectron microscopy, combined with myofibril mechanics, we determined the force-extension curve of the poly-Ig segment in situ. The relatively small dimensions of the myofibril preparation were advantageous in that they allowed extrapolation of the force down to the single molecule level and simulation of the experimental data by applying entropic

elasticity theory. On the other hand, a number of uncertainties in the data have to be considered. First, a critical step in the force analysis is the estimate of the true cross-sectional area of the specimens. In the past, this issue has been extensively dealt with (Bartoo et al., 1993; Linke et al., 1994): it was found that the variability in myofibrillar diameter, measured by light microscopy, may well reach ±20% of the average value (~1.0 μm), implying that the error in cross-sectional area measurements is even higher. Thus, a significant part of the nearly twofold variation in passive tension at a given SL (Fig. 6B) might be due to systematic error in the diameter estimates. However, with a large enough number of specimens used for the force measurements (>10), we think that the approach reveals valid estimates of passive tension. A second limitation of the analysis is due to the fact that even with protease inhibitors added to the buffer, titin degradation cannot be inhibited completely. Although the damage is limited (Fig. 2), it will affect force to some degree. Such effect cannot be adequately corrected for, because the magnitude of force reduction resulting from titin degradation may vary between experiments. Assuming that the relative force reduction is similar at all SLs, then the fit to WLC theory will still be valid, with the true persistence length being slightly overestimated. Finally, a third restriction to the calculation of force per titin also comes from the uncertainty as to how many titin strands exist per half thick filament, either three (e.g. Maruyama, 1994) or six (e.g. Whiting et al., 1989). From these results, we would argue that a 3:1 ratio is more likely, because a persistence length of 42 nm for a 6:1 (titin:half thick filament) ratio seems unreasonably large, compared to a contour length of 225 nm (cf. WLC theory; Marko and Siggia, 1995). Importantly, the uncertainty about the titin vs. thick filament ratio affects the calculation of a persistence length within a factor of two, but has no consequences for the fit quality. Altogether, the major conclusions of this study are valid regardless of the limitations to the force analysis.

Correct fits of the experimental data, for SLs far exceeding those found in vivo (range for psoas muscle, 2.2-3.2 μm; Goulding et al., 1997), were obtained with the entropic elasticity model according to Eq. 1 (Fig. 7). Thus, the N-terminal poly-Ig region may behave as a WLC over the entire physiological SL range, with A = 21 (42) nm. As for the value of 21 nm, a persistence length close to that found by us had earlier been reported by Higuchi et al. (1993) in a dynamic light scattering study on isolated titin molecules: the authors inferred a number of 15 nm. On the other hand, a mechanical study on single titin molecules has recently suggested a considerably smaller persistence length of ~5 nm for the Ig domain region (Tskhovrebova et al., 1997). This value, however, was deduced from modeling the force-extension relation of whole titin filaments and may not represent the true persistence length of the poly-Ig region. Whereas a value of 5 nm would indicate uncorrelated mechanical behaviour of individual Ig modules (length, ~4 nm; Whiting et al., 1989), this study's results instead suggest that stretches of at least 5-6 modules may be directionally correlated. Interestingly, it is known from sequence comparison that the skeletal muscle-specific Ig segments of I-band titin are arranged in repetitive patterns of several copies of 6 and 10 modules (Gautel, 1996). Considering the remarkable similarity in numbers, it appears that this clustering of Ig modules into super repeats could manifest itself as a mechanically cooperative behaviour, thereby defining the elasticity of the entropic spring. Further, the relatively low L:A ratio (probably ~10:1) for the poly-Ig region found in this study may point to a semiflexible chain that does not entirely collapse at zero stretch force. Thus, as suggested earlier (Linke et al., 1996), the elastic properties of the Ig regions may well be relevant in setting the physiological slack length of a sarcomere.

Finally, we note that the small forces of a few piconewtons per titin strand at low sarcomere stretch will make it difficult to experimentally prove the entropic spring concept for the poly-Ig region by measuring, for example, a possible temperature-dependency of force: the WLC model would predict that a temperature rise by 10 K (from 300 K) resulted in a force increase of only ~3%. When force increases more steeply during moderate sarcomere stretch, the analysis would become less straightforward, because then the extensibility of I-band titin is determined mainly by the PEVK element, not the poly-Ig region (Linke et al., 1996). As for the extreme sarcomere extensions, it is pointed out that the forces likely to induce unfolding of individual Ig modules (~35 pN for 3 titins/half thick filament, or half that value for a 6:1 ratio) have been deduced from the quasi steady-state passive length-tension relation. These values are similar to the forces of 20-40 pN found by Kellermayer et al. (1997). On the other hand, if we had used the peak tension at the end of a stretch (i.e. before the onset of stress relaxation; cf. Fig. 6A) to calculate the force-extension curve of a single titin, much greater unfolding forces, comparable to those reported by Tskhovrebova et al. (1997; ~100 pN), would have resulted. Even higher unfolding forces of 250-300 pN, as found by Rief et al. (1997), are difficult to explain by our findings. What appears to be clear, however, is that the forces needed to trigger Ig domain unfolding are stretch-rate dependent.

In summary, this study allows three main conclusions: first, a wormlike chain model can correctly simulate the elastic properties of the N-terminal poly-Ig segment of psoas muscle titin; second, titin's poly-Ig regions appear to behave as entropic springs over the entire range of physiological sarcomere lengths; and third, several adjacent Ig modules may take on orientations that are correlated, a finding perhaps related to the six-module or ten-module super repeat pattern within the Ig domain segments of skeletal muscle titin.

We thank J. C. Rüegg and W. Kriz for continuous support and S. Labeit and B. Kolmerer for helpful discussions. The financial support of the Deutsche Forschungsgemeinschaft (Li 690/2-1, SFB 320) is greatly acknowledged.

REFERENCES

Bartoo, M. L., Popov, V. I., Fearn, L. A. and Pollack, G. H. (1993). Active tension generation in isolated skeletal myofibrils. *J. Muscle Res. Cell Motil.* **14**, 498-510.

Bustamante, C., Marko, J. F., Siggia, E. D. and Smith, S. (1994). Entropic elasticity of λ-phage DNA. *Science* **265**, 1599-1600.

Erickson, H. P. (1994). Reversible unfolding of fibronectin type III and immunoglobulin domains provides the structural basis for stretch and elasticity of titin and fibronectin. *Proc. Nat. Acad. Sci. USA* **91**, 10114-10118.

Erickson, H. P. (1997). Stretching single protein molecules: titin is a weird spring. *Science* **276**, 1090-1092.

Fürst, D. O., Osborn, M., Nave, R. and Weber, K. (1988). The organization of titin filaments in the half-sarcomere revealed by monoclonal antibodies in immunoelectron microscopy: a map of ten nonrepetitive epitopes starting at the Z-line extends close to the M-line. *J. Cell Biol.* **106**, 1563-1572.

Gautel, M. (1996). The super-repeats of titin/connectin and their interactions: glimpses at sarcomeric assembly. *Advan. Biophys.* **33**, 27-37.

Gautel, M. and Goulding, D. (1996). A molecular map of titin/connectin elasticity reveals two different mechanisms acting in series. *FEBS Lett.* **385**, 11-14.

Goulding, D., Bullard, B. and Gautel, M. (1997). A survey of *in situ* sarcomere extension in mouse skeletal muscle. *J. Muscle Res. Cell Motil.* **18**, 465-472.

Granzier, H. L. and Irving, T. C. (1995). Passive tension in cardiac muscle: contribution of collagen, titin, microtubules and intermediate filaments. *Biophys. J.* **68**, 1027-1044.

Granzier, H., Helmes, M. and Trombitas, K. (1996). Nonuniform elasticity of titin in cardiac myocytes: a study using immunoelectron microscopy and cellular mechanics. *Biophys. J.* **70**, 430-442.

Higuchi, H., Nakauchi, Y., Maruyama, K. and Fujime, S. (1993). Characterization of β-connectin (titin 2) from striated muscle by dynamic light scattering. *Biophys. J.* **65**, 1906-1915.

Horowits, R., Kempner, E. S., Bisher, M. E. and Podolski, R. J. (1986). A physiological role for titin and nebulin in skeletal muscle. *Nature* **323**, 160-164.

Improta, S., Politou, A. S. and Pastore, A. (1996). Immunoglobulin-like modules from I-band titin: extensible components of muscle elasticity. *Structure* **4**, 323-337.

Itoh, Y., Suzuki, T., Kimura, S., Ohashi, K., Higuchi, H., Sawada, H., Shimizu, T., Shibata, M. and Maruyama, K. (1988). Extensible and less-extensible domains of connectin filaments in stretched vertebrate skeletal muscle as detected by immunofluorescence and immunoelectron microscopy using monoclonal antibodies. *J. Biochem. (Tokyo)* **104**, 504-508.

Kellermayer, M. S. Z., Smith, S. B., Granzier, H. L. and Bustamante, C. (1997). Folding-unfolding transitions in single titin molecules characterized with laser tweezers. *Science* **276**, 1112-1116.

Labeit, S. and Kolmerer, B. (1995). Titins, giant proteins in charge of muscle ultrastructure and elasticity. *Science* **270**, 293-296.

Labeit, S., Kolmerer, B. and Linke, W. A. (1997). The giant protein titin. Emerging roles in physiology and pathophysiology. *Circ. Res.* **80**, 290-294.

Linke, W. A., Popov, V. I. and Pollack, G. H. (1994). Passive and active tension in single cardiac myofibrils. *Biophys. J.* **67**, 782-792.

Linke, W. A., Ivemeyer, M., Olivieri, N., Kolmerer, B., Rüegg, J. C. and Labeit, S. (1996). Towards a molecular understanding of the elasticity of titin. *J. Mol. Biol.* **261**, 62-71.

Linke, W. A., Ivemeyer, M., Labeit, S., Hinssen, H., Rüegg, J. C. and Gautel, M. (1997). Actin-titin interaction in cardiac myofibrils: Probing a physiological role. *Biophys. J.* **73**, 905-919.

Marko, J. F. and Siggia, E. D. (1995). Stretching DNA. *Macromolecules* **28**, 8759-8770.

Maruyama, K. (1994). Connectin, an elastic protein of striated muscle. *Biophys. Chem.* **50**, 73-85.

Maruyama, K. (1997). Connectin/titin, giant elastic protein of muscle. *FASEB J.* **11**, 341-345.

Mundel, P., Gilbert, P. and Kriz, W. (1991). Podocytes in glomerulus of rat kidney express a characteristic 44 kD protein. *J. Histochem. Cytochem.* **39**, 1047-1056.

Rief, M., Gautel, M., Oesterhelt, F., Fernandez, J. M. and Gaub, H. E. (1997). Reversible unfolding of individual titin immunoglobulin domains by AFM. *Science* **276**, 1109-1112.

Smith, S. B., Cui, Y. and Bustamante, C. (1996). Overstretching B-DNA: the elastic response of individual double-stranded and single-stranded DNA molecules. *Science* **271**, 795-799.

Tatsumi, R. and Hattori, A. (1995). Detection of giant myofibrillar proteins connectin and nebulin by electrophoresis in 2% polyacrylamide slab gels strengthened with agarose. *Anal. Biochem.* **224**, 28-31.

Tokuyasu, K. T. (1989). Use of poly(vinylpyrrolidone) and poly(vinyl alcohol) for cryoultramicrotomy. *Histochem. J.* **21**, 163-171.

Trinick, J. (1994). Titin and nebulin: protein rulers in muscle? *Trends Biochem. Sci.* **19**, 405-409.

Trombitas, K., Baatsen, P. H. W. W., Kellermayer, M. S. Z. and Pollack, G. H. (1991). Nature and origin of gap filaments in striated muscle. *J. Cell Sci.* **100**, 809-814.

Trombitas, K. and Pollack, G. H. (1993). Elastic properties of the titin filament in the Z-line region of vertebrate striated muscle. *J. Muscle Res. Cell Motil.* **14**, 416-422.

Tskhovrebova, L., Trinick, J., Sleep, J. A. and Simmons, R. M. (1997). Elasticity and unfolding of single molecules of the giant muscle protein titin. *Nature* **387**, 308-312.

Wang, K., McCarter, R., Wright, J., Beverly, J. and Ramirez-Mitchell, R. (1991). Regulation of skeletal muscle stiffness and elasticity by titin isoforms: A test of the segmental extension model of resting tension. *Proc. Nat. Acad. Sci. USA* **88**, 7101-7105.

Wang, K., McCarter, R., Wright, J., Beverly, J. and Ramirez-Mitchell, R. (1993). Viscoelasticity of the sarcomere matrix of skeletal muscles; the titin-myosin composite filament is a dual-stage molecular spring. *Biophys. J.* **64**, 1161-1177.

Whiting, A., Wardale, J. and Trinick, J. (1989). Does titin regulate the length of muscle thick filaments? *J. Mol. Biol.* **205**, 263-268.